EPJ AP

Applied Physics

EPJ.org
your physics journal

Eur. Phys. J. Appl. Phys. (2015) 70: 20103 DOI: 10.1051/epjap/2015140205

Radiation polarization of silicon carbide p-n-structures, operating in electrical breakdown regime

Aleksey M. Genkin, Vera K. Genkina, and Svetlana M. Zubkova

edp sciences

The title "The European Physical Journal" is a joint property of EDP Sciences, Società Italiana di Fisica (SIF) and Springer

Eur. Phys. J. Appl. Phys. (2015) 70: 20103
DOI: 10.1051/epjap/2015140205

THE EUROPEAN PHYSICAL JOURNAL
APPLIED PHYSICS

Regular Article

Radiation polarization of silicon carbide p-n-structures, operating in electrical breakdown regime

Aleksey M. Genkin[1], Vera K. Genkina[1], and Svetlana M. Zubkova[2,a]

[1] National Technical University of Ukraine "Kyiv Polytechnical Institute", 03056 Kyiv, Ukraine
[2] I.N. Frantzevich Institute for Problems of Materials Science of National Academy of Sciences of Ukraine, 03142 Kyiv, Ukraine

Received: 11 May 2014 / Received in final form: 22 September 2014 / Accepted: 8 April 2015
Published online: 19 May 2015 –

Abstract. The spectral dependence of the linear polarization degree of the electroluminescence that accompanies the electrical breakdown of the alloyed *p*-*n*-structures prepared on the basis of 4H-, 6H-, 15R-, and 3C-SiC polytypes in the region of 1.4–3.8 eV has been obtained. The structures were located on the crystal faces parallel and perpendicular to the crystallographic **C**-axis. The radiation was extracted from a thin *p*-region at an acute angle and also perpendicular to a working face of a crystal. The radiation components which were linearly polarized in the planes parallel and perpendicular to the crystallographic **C**-axis ($\mathbf{E}\|\mathbf{C}$, $\mathbf{E}\perp\mathbf{C}$) and parallel to the vector **F** of the electric field intensity ($\mathbf{E}\|\mathbf{F}$) in a *p*-*n*-junction have been revealed. It turned out that the spectrum position and the intensity of the components associated with the **C**-axis direction differ essentially depending on the polytypes. It has been revealed that the presence of the radiation polarization with the degree of 0.3–0.4 in the plane $\mathbf{E}\|\mathbf{C}$ in the fundamental absorption region and in the adjacent region is common for all polytypes. Only in 6H- and 15R-SiC polytypes did the optical absorption data correspond to the radiation polarization characteristics. The polarization $\mathbf{E}\|\mathbf{F}$ achieved the degree of 0.5 and had a tendency to increase towards the higher photon energies.

1 Introduction

At present the original phenomena associated with the presence of a superlattice that occurs at high electric fields in SiC polytypes, attract a considerable scientific and practical interest (e.g., [1,2]). It is known, that the presence of a natural superlattice in silicon carbide polytypes causes the minizone structure in the conduction band, which leads to a number of effects such as a negative differential conduction in the Bloch oscillation regime, Stark-phonon resonances, a low minizone localization, a resonance tunneling between minizones, a monopolar hole impact ionization in a wide field region, anomalous high breakdown fields with a negative temperature dependence of the breakdown voltage and a lot of other new effects.

In order to understand the nature of the physical processes underlying these phenomena it may require more delicate and precise experiments to obtain new experimental data. It is the electroluminescence which accompanies the electrical breakdown in a *p*-*n*-junction, the so-called breakdown electroluminescence (BEL), that may become a source of the useful information. The BEL in SiC crystals has also a practical application for creating highly stable, broadband, high-speed light emitting diodes (LED) (e.g., [3,4]).

[a] e-mail: smzubkova@gmail.com

A significant anisotropy of SiC crystals may result in the BEL polarization with respect to the direction of the crystallographic **C**-axis. The BEL polarization with respect to the vector of the electric field intensity **F** in a *p*-*n*-junction is also possible.

The difference between the BEL spectral characteristics for two mutually orthogonal (parallel and perpendicular to the **C**-axis of an α-SiC crystal) positions of a polarizing prism for 6H-SiC-based *p*-*n*-structures was described in reference [5]. The BEL for the 6H-SiC-based diodes was shown to contain bands in the neighbourhood of 1.5 and 3.3 eV with the polarization $\mathbf{E}\|\mathbf{C}$, where **E** is a vector of the electrical field intensity of the electromagnetic wave. The spectral distribution of the BEL polarization degree in 6H-SiC-based *p*-*n*-structures was also obtained in reference [6]. The received data confirmed the presence of the bands with the polarization $\mathbf{E}\|\mathbf{C}$. The band with the polarization $\mathbf{E}\perp\mathbf{C}$ was also detected near 2.6 eV. The authors observed an equivalence of polarization characteristics of the *p*-*n*-structures that had been prepared on the crystal faces, corresponding to the crystallographic directions which were perpendicular to the **C**-axis.

Unfortunately, there has not been any sufficient information concerning the BEL polarization up to now. In particular, the spectral dependence the polarization degree of the BEL with respect to the **C**-axis has been obtained only for a 6H-SiC sample [6]. However, we do not know any BEL polarization data in semiconductor structures with respect to the vector of the breakdown electric field intensity. The investigation of the BEL polarization of the different SiC polytypes with respect to **C**-axis and to the electric field intensity vector **F** in a *p*-*n*-junction will provide the important information about the crystal structure polytypes influence on electronic processes in the breakdown electric fields as well as their BEL mechanisms. It will also contribute to the creation of new elements for photonic application – the highly stable sources of optical radiation with a controlled polarization state.

The present paper is dedicated to the detailed investigation of the BEL polarization characteristics and the polytype crystal structure effect on them, as well as the electrical breakdown nature, the sample powering regime and other factors. The possible practical applications of the radiation polarization have also been investigated.

2 Experimental technique

We investigated the *p*-*n*-junctions prepared by alloying silumin (Al + Si) in 4H-, 6H-, 15R- and 3C-SiC crystals. Those *p*-*n*-junctions were prepared on the natural crystal faces perpendicular to the crystallographic **C**-axis, and also on the end faces parallel to the **C**-axis. The end faces were prepared by cutting and polishing the thick crystals. It should be noted that it was impossible to improve the surface quality of the end faces by chemical etching in KOH-based melts. So, their quality was much worse than the quality of the natural faces. The samples being used had microplasmas which differed slightly in turn-on voltage and were ringed round the vicinity of the *p*-*n*-junction. In the case of the 3C-SiC crystal the microplasmas were localized along a narrow ring in the *p*-*n*-structure periphery. The radiation was extracted through a thin *p*-region. Measurements were carried out at values of the applied current 50 and 100 mA.

The methods of extracting the radiation of the samples being used by us while investigating the BEL polarization are shown in Figure 1. In the methods 1 and 4 the *p*-*n*-structures were placed on the artificial crystal faces parallel to the **C**-axis, and in the methods 2 and 3 – on the natural faces perpendicular to the **C**-axis. Method 3 allowed us to observe (to the certain accuracy) the total radiation polarization with respect to vectors **F** and **C**.

Taking into account that there was a much wider choice of the samples with high quality *p*-*n*-structures prepared on the natural crystal faces as contrasted to those with *p*-*n*-structures prepared on the artificial faces parallel to the **C**-axis, the method 3 was mainly used. This method also allowed us to observe the BEL polarization of the cubic 3C-SiC crystal with respect to the vector **F**. It is necessary to note that the 3C-SiC crystal does not have a natural superlattice as well as a respective anisotropy. Besides, the types of the breakdown in the directions of the electric field $\mathbf{F}\perp\mathbf{C}$ (on the end crystal faces) and $\mathbf{F}\|\mathbf{C}$ (on the natural crystal faces) vary considerably [1].

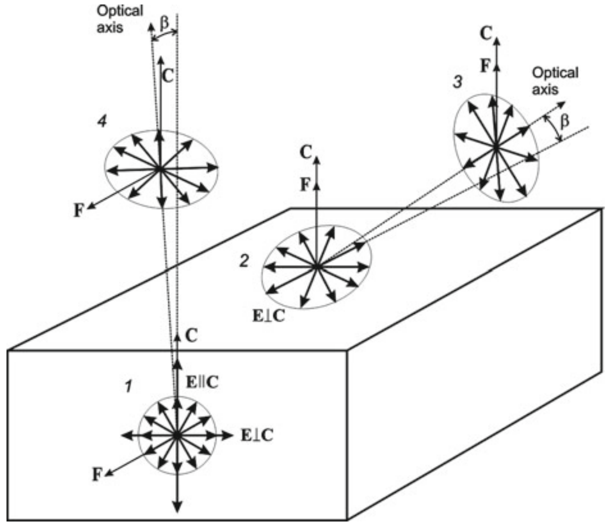

Fig. 1. Schema of the radiation extraction. The directions of the optical axis of the recording system: (1) axis is perpendicular to the face plane and to the vector **C** as well as is parallel to the vector **F**; (2) axis is perpendicular to the face plane and is parallel to vectors **F** and **C**; (3) axis is directed at the acute angle of β to the face plane and at the angle of $(\pi/2-\beta)$ – to the **C**-axis and to the vector **F**; (4) axis is directed at the acute angle of β to the face plane, and to the **C**-axis and at the angle of $(\pi/2-\beta)$ – to the vector **F**.

The last case ($\mathbf{F}\|\mathbf{C}$) is of a practical interest for creating original devices. Therefore, the method 3 is the only way to estimate the spectral dependence of the BEL polarization degree with respect to vectors **C** and **F** for the *p*-*n*-structures prepared on the natural crystal faces.

The method 4 allowed us to observe the radiation polarization of the end samples mainly with respect to the vector **F**. In order to reduce the influence of the radiation polarization with respect to the crystallographic **C**-axis it was necessary to center a sample so that the optical axis of the recording system and the **C**-axis were arranged at the same plane. The BEL polarization state was determined from the measured values of the intensity of the radiation, transmitted through a polarizer at four fixed values of a rotation angle (in the device reference system) 0, 45, 90 and 135 °C. In our case, we could expect the simultaneous presence of two mutually orthogonal incoherent components ($\mathbf{E}\perp\mathbf{C}$ and $\mathbf{E}\|\mathbf{C}$). An analysis of the total radiation polarization did not allow intensities of each component to be obtained separately. Actually, in this case the dependence of the radiation intensity I (on the polarizer output) on the polarizer rotation angle of α may be written as follows:

$$I(\alpha) = I_1\cos^2(\alpha-\varphi) + I_2\sin^2(\alpha-\varphi) + \frac{1}{2}I_0 = (I_1 - I_2)\cos^2(\alpha-\varphi) + I_2 + \frac{1}{2}I_0, \quad (1)$$

where I_1 is the radiation component intensity with the polarization plane located at an angle of φ in the device reference system; I_2 is the radiation component intensity with the polarization plane located at an angle of $(\varphi \pm \pi/2)$; I_0 is the intensity of the unpolarized radiation component.

Thus, the total radiation does not differ from a mixture of component with the intensity $(I_1 - I_2)$ with the polarization plane corresponding to an angle of φ in the device reference system, and unpolarized radiation component with the intensity $(2I_2 + I_0)$.

In this case, the measured values I^k (the index k corresponds to the rotation angle of α) allowed us to determine the polarization parameters such as the difference of the intensities of linearly polarized components $(I_1 - I_2)$, the summary intensity of the radiation $(I = I_1 + I_2 + I_0)$ as well as the angle of φ of the polarization plane.

For the values of the measured intensities I^k we can write:

$$I^0 = I_1 \cos^2\varphi + I_2 \sin^2\varphi + \frac{1}{2}I_0, \quad (2)$$

$$I^{45} = I_1 \cos^2(\varphi - 45°) + I_2 \sin^2(\varphi - 45°) + \frac{1}{2}I_0, \quad (3)$$

$$I^{90} = I_1 \sin^2\varphi + I_2 \cos^2\varphi + \frac{1}{2}I_0, \quad (4)$$

$$I^{135} = I_1 \sin^2(\varphi - 45°) + I_2 \cos^2(\varphi - 45°) + \frac{1}{2}I_0. \quad (5)$$

Whence it follows that:

$$\varphi = \frac{1}{2}\mathrm{arctg}\left(\frac{I^{45} - I^{135}}{I^0 - I^{90}}\right), \quad (6)$$

$$I = (I^0 + I^{90} + I^{45} + I^{135})/2, \quad (7)$$

$$I_1 - I_2 = [(I^0 - I^{90})^2 + (I^{45} - I^{135})^2]^{0,5}. \quad (8)$$

The degree of the radiation polarization was determined by the formula:

$$P = \frac{I_1 - I_2}{I}. \quad (9)$$

In cases of $\mathbf{E}\|\mathbf{C}$ and $\mathbf{E}\|\mathbf{F}$ the value of P was taken as positive and in case of $\mathbf{E}\perp\mathbf{C}$ value of P was taken as negative.

Further the calculated dependence (1) was compared with the experimental results in order to estimate the accuracy in the determination of polarization parameters. The results obtained for one of the samples on 6H-SiC-based (the method 1 of the radiation extraction) are shown in Figure 2. Two mutually orthogonal linearly polarized components $\mathbf{E}\perp\mathbf{C}$ and $\mathbf{E}\|\mathbf{C}$ have been revealed for this sample. As one can see from Figure 2 the phase of the angular dependence is the same at the wavelengths 361.5 nm and 687 nm and it varies by 90° at the wavelength 474 nm. This fact indicates the predominance of the spectral band with the perpendicular direction of the polarization plane. Such a good similarity of the calculated and experimental dependences has been also observed for the other samples.

We used a set of interference light filters for the emission monochromatisation. The sample was placed on a special rotating unit. This unit made it possible to change an angle of β between the p-n-junction plane and the optical axis of the recording system. The influence of the radiation reflected from the crystal faces was decreased by covering the corresponding areas with light-absorbing paint. The radiation of the sample under study passed subsequently through an interference filter, an aperture diaphragm, an optical shutter, a polarizer and a photomultiplier operating in a photon-counting regime. The aperture diaphragm angle did not exceed 3°. A polaroid was used as a polarizer. It was placed in a hermetic rotating unit with a scale graduated in degrees. The parts of the experimental unit were placed on a massive metal base. It was possible to change samples and filters, to regulate

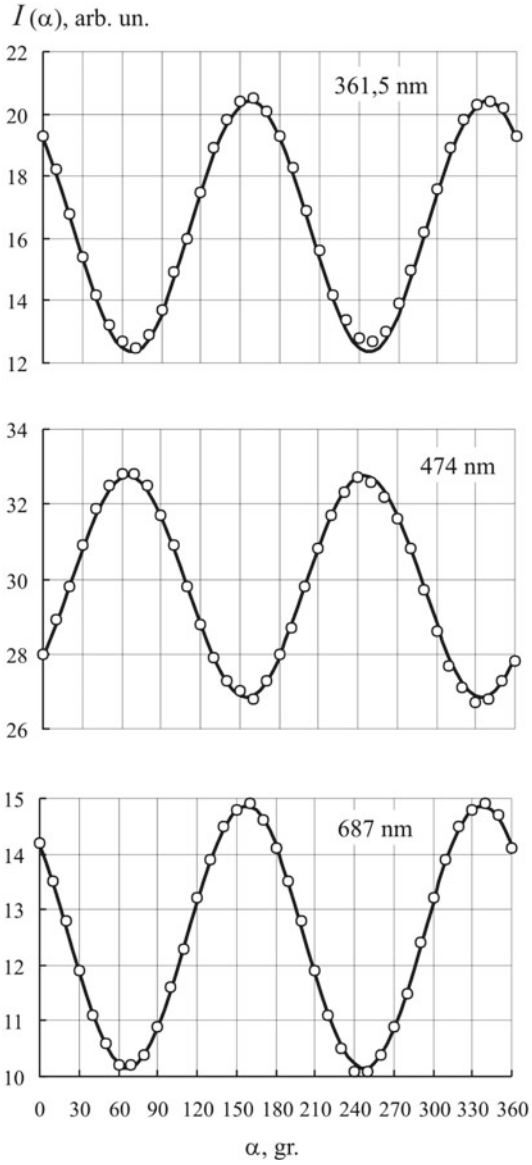

Fig. 2. Dependence of the photomultiplier signal on the rotation angle of the analyzer for different wavelength values: points – experimental results; solid curve – calculation by formula (1) with using parameters obtained by formulas (6)–(8).

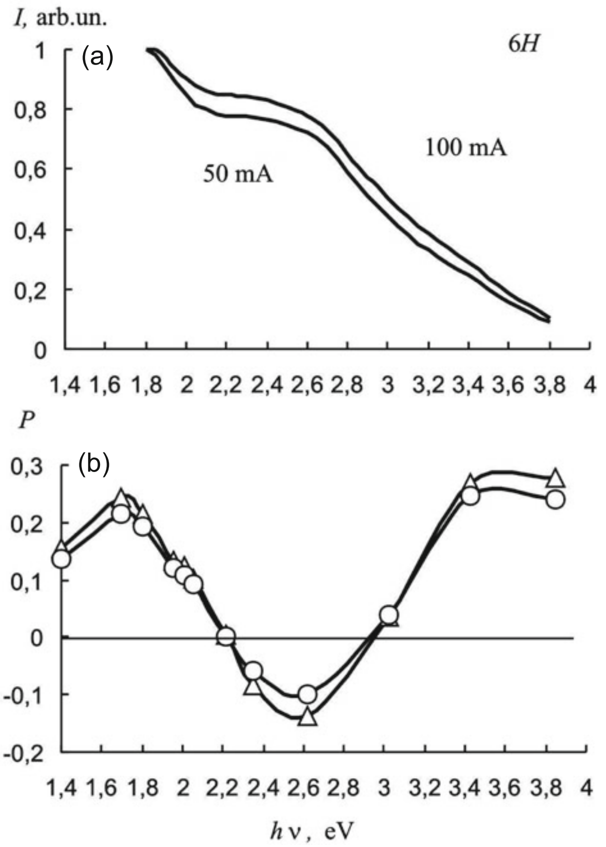

Fig. 3. Spectral dependence of the intensity (a) and of the polarization degree (b) for the 6H-SiC based sample radiation. The method of the emission extraction is 1. The sample powering regimes are: *Δ* – 50 mA, 14,9 V; O – 100 mA, 18,5 V.

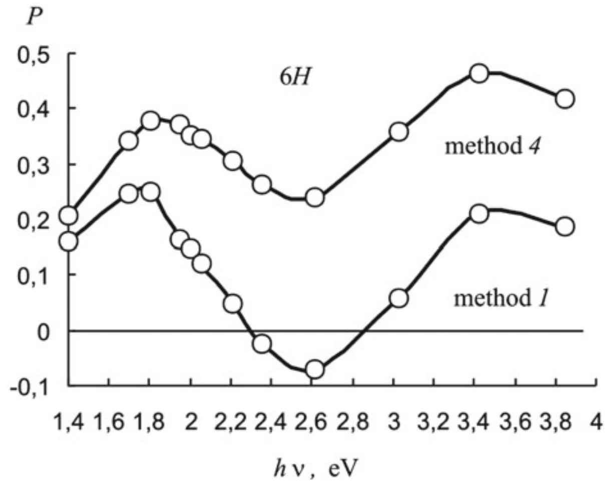

Fig. 4. Spectral distribution of the polarization degree for the 6H-SiC-based sample in two methods of the radiation extraction. The sample powering regime is: 100 mA, 26 V.

a rotation angle of the polarizer in external lighting without turning off a power supply of the photomultiplier.

The radiation of the *p-n*-structures prepared on the natural 6H-SiC crystal face which was perpendicular to the **C**-axis (Fig. 1, method 2) was being recorded in order to estimate an accuracy of the determination of the polarization degree associated with the effect of the parts of the experimental unit. The polarization should not be observed when extracting the emission by this method. The experimental values of the polarization degree *P* of the radiation for the mentioned above samples appeared not to exceed 2% at the different wavelength values.

The spectral distribution of an integral intensity of the unpolarized radiation has been measured by using a mirror prism monochromator. The corresponding plots are scaled in proportion to the number of photons emitted within a single interval of the photon energy.

3 Experimental results

The data for a typical 6H-SiC-based *p-n*-structure sample prepared on an artificial end face are shown in Figure 3. As one can see from this figure, there are the radiation components with polarization **E**‖**C** and **E**⊥**C** near 2.6 eV. When reducing the current supplied from 100 to 50 mA the polarization degree increases appreciably.

The data for a sample on the 6H-SiC base, in which the *p-n*-junction was prepared on a cleavage face parallel to the **C**-axis, are shown in Figure 4. The surface of this face was of high quality. The sample contained a uniform field of microplasmas with a minor spread of the breakdown voltages. The data have been obtained when the radiation was being extracted by two different methods while the power regime was identical.

As one can see from the Figure 4 the character of the spectral distribution in the case of the method 4 remains the same. This fact indicates the effect of polarization with respect to the **C**-axis, however, there is the significant background polarization at the plane **E**‖**F**.

The samples in Figures 3 and 4 differ considerably in the values of the operating voltage. At the same time a significant difference in the characters of the spectral distributions of the polarization degree has not been detected.

Figure 5 shows the data for a typical sample based on the 6H-SiC crystal. Its *p-n*-junction was prepared on a natural crystal face (the method 3 of the emission extraction). The characteristics of this sample are optimal for using it as a reference emitter [3].

A relatively small degree of a total polarization (**E**‖**F**, **E**‖**C**) and its decay in the lower photon energy range are typical for such samples.

The data for a sample on the 15R-SiC base are shown in Figure 6. The *p-n*-junction for this sample was placed on an artificial end face. As one can see from Figure 6 there is a relatively narrow component with polarization **E**‖**C**, which has a maximum in the range of 1.8–2.0 eV. At the edge of the spectrum (1.4 eV) the polarization is practically absent. The spectral band with polarization **E**⊥**C** compared with that of SiC-6H-based sample is shifted significantly towards the lower photon energies. Besides, the general polarization degree of the radiation is lower than that of the 6H-SiC-based sample.

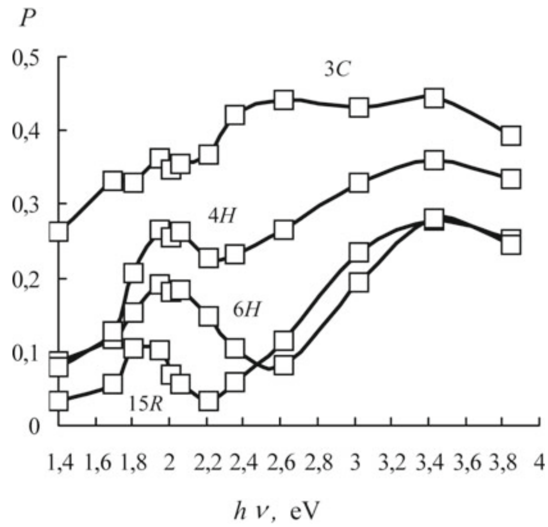

Fig. 5. Spectral distribution of the polarization degree for the samples on the basis of different SiC polytypes. The method of the emission extraction for polytypes: 3C-, 6H-, 15R-SiC is 3, for 4H-SiC crystal is 4. The samples powering regimes for different polytypes are: 15R – 50 mA, 17 V; 6H – 100 mA, 17 V; 4H – 100 mA, 23 V; 3C – 100 mA, 21 V.

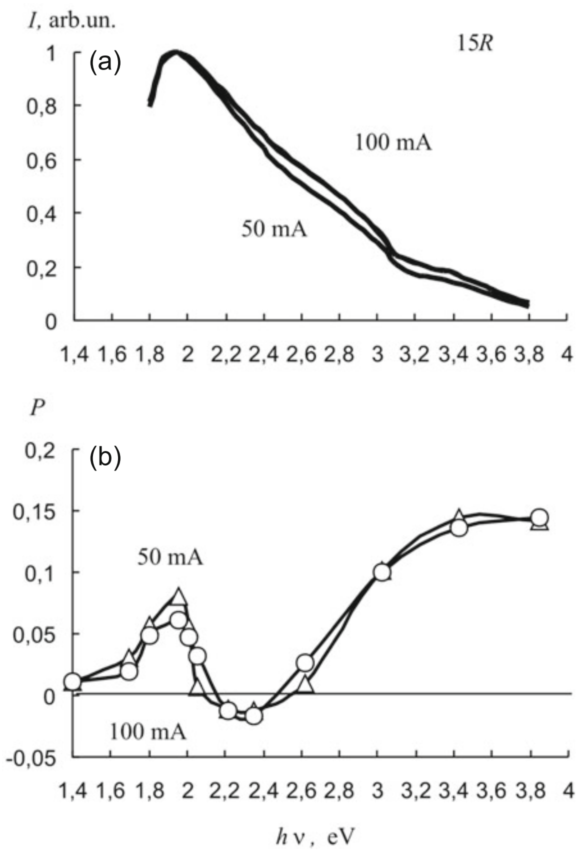

Fig. 6. Spectral dependence of the intensity (a) and of the polarization degree (b) of the 15R-SiC based sample radiation. The method of the emission extraction is 1. The sample powering regimes are: Δ – 50 mA, 20,9 V; O – 100 mA, 21,7 V.

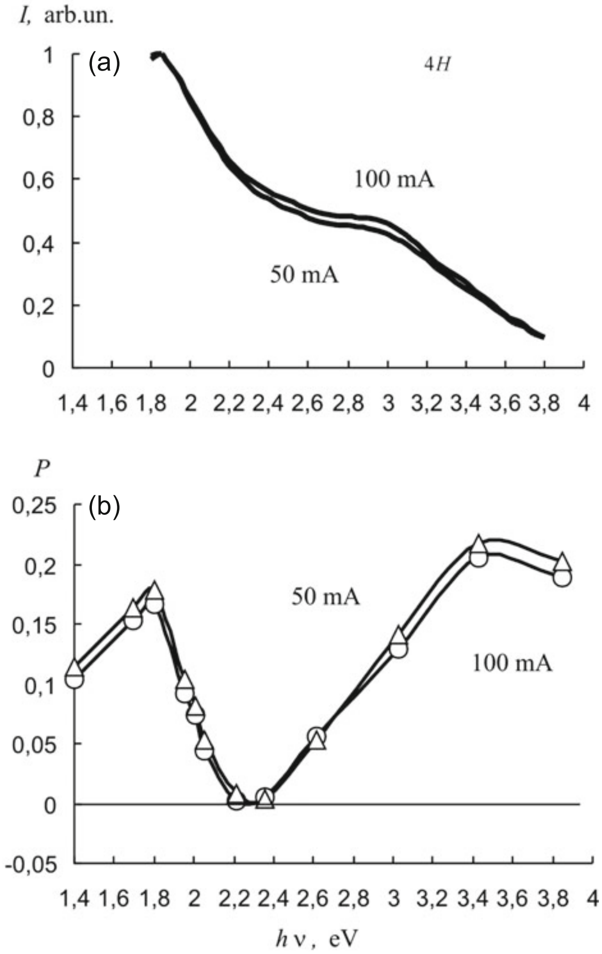

Fig. 7. Spectral dependence of the intensity (a) and of the polarization degree (b) of the 4H-SiC-based sample radiation. The method of the emission extraction is 1. The sample powering regimes are: Δ – 50 mA, 17,6 V; O – 100 mA, 19,2 V.

Furthermore, a significant dependence on a feed current is not observed.

The data for a typical sample based on the 15R-SiC crystal, its *p*-*n*-junction being placed on a crystal natural face, are shown in Figure 5. The radiation was extracted by the method 3 in this case.

A character of the spectral distribution of the total polarization ($\mathbf{E}\|\mathbf{F}$, $\mathbf{E}\|\mathbf{C}$) is similar to that in Figure 6. However, the total polarization increases considerably in the range of the high photon energies.

The data for a typical sample based on the 4H-SiC crystal are shown in Figure 7. The *p*-*n*-junction for this sample was located on the artificial end face. As one can see from Figure 7, there is an energy dip in the middle part of the spectral distribution at 2.2 eV, which is shifted by approximately 0.4 eV towards the lower photon energies as compared with the 6H-SiC crystal in Figure 3. The spectral band with the polarization $\mathbf{E}\perp\mathbf{C}$ appears to take place on the site of this dip for lots of samples. Just as for the 6H-SiC-based *p*-*n*-junction, a marked increase of a polarization degree has been observed with a decrease of a feed current.

As it is seen from Figure 7 in case of the 4H-SiC sample the polarization degree with respect to the vector **F** (method 4 of the radiation extraction (Fig. 5)) increases considerably towards the higher photon energies. An effect of the polarization with respect to the **C**-axis seems to manifest itself as a maximum in the vicinity of 2 eV, which is slightly shifted as compared with Figure 7 due to increasing the general spectral distribution towards the higher photon energies.

The data concerning the polarization with respect to the vector **F** for the 3C-SiC sample in the method 3 are shown in Figure 5. The significant radiation polarization in the plane $\mathbf{E}\|\mathbf{F}$, the weak structure and the increase of the spectral distribution towards the higher photon energies have been observed in this case.

4 Discussion

The breakdown electroluminescence in silicon carbide is historically the first known type (Losev, 1927) of the solid-state electroluminescence. The BEL spectra in SiC consist of the broad bands with a weak structure. However, the BEL phenomenon has not yet unambiguously explained up to now. For example, in reference [7] the BEL spectra is associated with the indirect transitions of the high-energy electrons. In this case the impurity bands of the recombination radiation in the quasi-neutral base are used to explain the features of the spectrum in the visible region. According to another view, the BEL is associated with the direct transitions of the high-energy holes between the subbands of a valence band [8]. In a cubic 3C-SiC the narrow intense band was observed on the background of a wide spectrum in the vicinity of 3.1 eV. The presence of this band is supposed to be due to the transitions of high-energy electrons from the overlying subband [9].

Results obtained for a number of SiC polytypes demonstrate a presence of a significant, spectrum-dependent, linear polarization of the BEL in the planes parallel and perpendicular to the crystallographic axis **C** and parallel to the vector **F** of the electric field intensity in a *p-n*-junction.

The spectral dependence of the polarization degree associated with the **C**-axis direction has a similar character for the different polytypes, but there are also significant differences, mainly in a spectral position of these dependence features.

A similarity takes place in the region of the high photon energies, where the polarization degree ($\mathbf{E}\|\mathbf{C}$) tends to increase towards relatively high values. The region of small values of the polarization degree in the perpendicular plane ($\mathbf{E}\perp\mathbf{C}$) is typical for a central part of the spectral dependence. The polarization in the plane parallel to the **C**-axis ($\mathbf{E}\|\mathbf{C}$) has been observed at the lower photon energies. It should be noted that the shape of the spectral distribution of the polarization degree associated with the **C**-axis direction for the 6H-SiC crystal is quite similar to the data obtained in reference [6]. Although, there are significant differences in a spectral dependence of the polarization degree for 6H- and 15R-SiC polytypes (Figs. 3 and 6). In particular, in case of the 6H-SiC crystal in the range of the lower photon energies we have observed the relatively high polarization degree in the form of a band with a maximum near 1.7 eV, which continued towards the lower energy values. At the same time in the case of 15R-SiC crystal a relatively narrow band with a maximum at 1.9 eV has been observed. For the 15R-SiC crystal the band with polarization $\mathbf{E}\perp\mathbf{C}$ has a maximum near 2.3 eV, while for the 6H-SiC crystal it is near 2.6 eV.

For the polytype 4H-SiC (Fig. 7) the band with a significant polarization in the range of the lower photon energies is markedly shifted as compared with the 6H-SiC crystal towards the higher energies and has a maximum near 1.8 eV. A central minimum of the spectral dependence near 2.3 eV is shifted significantly towards the lower energies.

It is interesting to compare the obtained data with the available absorption information, since the absorption and emission processes are connected with each other. Two of the above-mentioned bands (1.7 eV in the 6H-SiC crystal and 1.9 eV in the 15R-SiC crystal) have the spectral positions which are similar to the properly polarized bands of an optical absorption [10]. The presence of these bands is caused by the direct electron transitions between mini-bands in the conduction band. We can therefore assume that the radiation bands are due to reverse transitions. To our surprise the similar optical absorption band (with a maximum near 2.1 eV) for the 4H-SiC crystal [10] does not correspond to the energy position of the emission band in the range of 1.8 eV (Fig. 7).

An existence of the significant polarization in the plane $\mathbf{E}\|\mathbf{C}$ in the fundamental absorption region for the 6H-SiC crystal correlates with the optical absorption data from [10], those absorption having the same polarization in the corresponding spectral region. Therefore, the radiation polarization for the 6H-SiC in the fundamental absorption region can be explained by the anisotropy of the probability of the radiative transitions.

The bands in the central part of the spectral distribution (polarized in the plane $\mathbf{E}\perp\mathbf{C}$) are not associated with the corresponding bands in the optical absorption spectra. Therefore, it is possible to assume [6] that their appearance is caused by the anisotropic centers of radiation such as donor-acceptor pairs.

The smaller values of the polarization degree for the structures prepared on the natural 6H-SiC crystal faces perpendicular to the **C**-axis as opposed to the end faces may indicate an effect of the different types of electrical breakdown at these faces on the BEL characteristics. In particular, when the direction of the electric field in the *p-n*-junction is $\mathbf{F}\|\mathbf{C}$ (for the natural crystal faces) the electrons heating by the electric field is suppressed by the influence of the minizone structure in the conduction band. In this case, we can expect a decrease of ordering in the quasi-impulses direction of the high-energy electrons [1].

The obtained data demonstrate the presence of the significant BEL polarization associated with the direction of the electric field strength **F** in a *p*-*n*-junction. It is easy to view the polarization effect under a microscope using a polaroid. As a rule, the polarization degree in the plane $\mathbf{E}\|\mathbf{F}$ tends to increase towards the higher photon energies. Such a tendency is obvious for the samples based on the 15R- and 4H-SiC crystals (Fig. 5). This effect may indicate a higher degree of ordering in the directions of quasi-impulses of high energy current carriers.

5 Conclusions

We have carried out a detailed investigation of the polytypes 6H-, 4H-, 15R- and 3C-SiC-spectral dependence of the linear polarization degree of the electroluminescence, that accompanies the electrical breakdown in alloyed *p*-*n*-junctions. The radiation components polarized in the planes parallel and perpendicular to the crystallographic **C**-axis ($\mathbf{E}\|\mathbf{C}$, $\mathbf{E}\perp\mathbf{C}$) have been revealed. The polarization in the plane parallel to the vector **F** of the electric field intensity in the *p*-*n*-junction ($\mathbf{E}\|\mathbf{F}$) was observed. The spectral position and the intensity of the components associated with the **C**-axis direction differ significantly in the different polytypes. Polarization characteristics of the radiation correspond to the optical absorption data only in some cases. Polarization $\mathbf{E}\|\mathbf{F}$ tends to increase towards the higher photon energies.

It is possible that the considerable linear polarization of highly stable LEDs, which takes place in certain cases, may have a practical application.

References

1. V.I. Sankin, Semiconductor **36**, 717 (2002)
2. V.I. Sankin, A.V. Andrianov, A.O. Zakhar, A.G. Petrov, JETP Letters **94**, 362 (2011)
3. A.M. Genkin, V.K. Genkina, L.P. Germash, Tech. Phys. **44**, 1191 (1999)
4. A.M. Genkin, V.K. Genkina, L.P. Germash, Tech. Phys. **45**, 432 (2000)
5. Yu.M. Altayiskyi, A.M. Genkin, Sov. Phys. Semiconductors **14**, 827 (1980)
6. V.V. Guts, I.V. Malimon, I.V. Solonchuk, J. Appl. Spectrosc. **46**, 153 (1987)
7. L.A. Kosyachenko, A.V. Pivovar, V.M. Sklyarchuk, J. Appl. Spectrosc. **36**, 178 (1982)
8. A.O. Kostantinov, Semiconductor **21**, 670 (1987)
9. M.V. Belous, A.M. Genkin, V.K. Genkina, O.A. Guseva, Semiconductors **31**, 169 (1997)
10. G.V. Dubrovskii, A.A. Lepneva, E.I. Radovanova, Phys. Stat. Sol. B **57**, 423 (1973)